Determination of the Structure of a Novel Anion Exchange Fuel Cell Membrane by Solid-State Nuclear Magnetic Resonance Spectroscopy

Xueqian Kong, Kuldeep Wadhwa, John G. Verkade, and Klaus Schmidt-Rohr*

Department of Chemistry and Ames Laboratory, Iowa State University, Ames, Iowa 50011

Received November 20, 2008; Revised Manuscript Received January 17, 2009

ABSTRACT: A novel anion exchange fuel cell membrane was successfully synthesized by chemically attaching proazaphosphatranium/phosphatranium cations under microwave treatment to the sulfonic groups of Nafion-F. Solid-state nuclear magnetic resonance (NMR) techniques were employed to determine the actual structure and composition of this anion exchange membrane. ^{31}P NMR showed two main signals with a 2:1 intensity ratio and chemical shift changes of +89 and +46 ppm, respectively, from the main peak of phosphatranium chloride. ^{1}H−^{31}P heteronuclear correlation (HetCor) NMR and ^{1}H−^{31}P recoupling experiments indicated that the proton originally bonded to phosphorus in phosphatranium chloride is replaced in the major component of the Nafion−proazaphosphatranium/phosphatranium composite. ^{19}F NMR experiments showed that the fluorine in the −SO_2F group of the Nafion-F precursor is fully replaced. ^{31}P{^{19}F} rotational-echo double-resonance (REDOR) experiments measured a P−F internuclear distance of ∼0.4 nm, which showed that the proazaphosphatranium is covalently attached to Nafion through a S−P bond. ^{13}C NMR and ^{1}H−^{13}C HetCor spectra indicated that the proazaphosphatranium structure is maintained even after the microwave treatment at 180 °C and also showed indications of entrapped dimethylformamide solvent.

Introduction

The increasing demand for alternative sources of energy[1−4] has placed direct methanol-based fuel cells (DMFCs) at the forefront of the search for alternatives to fossil fuels. DMFCs are projected to be the first fuel cells that will be commercially available for use by the general population. Among the advantages of DMFCs are their high energy density (5−10 times greater than that of commonly available batteries), moderate operating temperatures, and easy replacement of the methanol fuel cartridge, all of which make DMFCs ideal for usage in portable electronic devices.[5−7] In many modern fuel cells, a proton exchange membrane (PEM) is utilized to transport protons produced in the anodic half-reaction for consumption on the cathodic side of the cell (Scheme 1a). However, PEMs in DMFCs suffer from (i) parasitic crossover of methanol, which leads to a lowering of cell voltage and efficiency; (ii) electro-osmosis of water from anode to cathode, which causes severe flooding at the cathode; and (iii) reduced catalyst kinetics in the acidic environment requiring high loadings of costly precious-metal catalysts, e.g., platinum.[8] For these reasons, alkaline fuel cells (AFCs) with the same net reaction but exploiting different half-reactions as shown in Scheme 1b have become attractive to investigate. The most important advantages of AFCs are that they can operate at a lower catalyst loading owing to more facile methanol oxidation in alkaline media[9−11] and that they may utilize a broader range of catalysts, such as nickel and silver.[12−14]

In the past, methanol was not suitable as a fuel in AFCs because such cells utilized liquid alkaline electrolytes such as hydroxide ion conductors, which are vulnerable to precipitation of carbonate (e.g., K_2CO_3) that destroys the catalyst layer, which forms from CO_2 released in the cell reaction (Scheme 1b).[15−17] As a result, solid alkaline anion exchange membranes (AAEMs) containing hydroxide ions were developed. They combine the advantages of PEMs (flexibility, durability, small volume, and no leakage) and traditional AFCs (good catalyst kinetics), and they can operate when carbonate species are present.[8] Some efforts have been made to use fluorinated polymers as AAEMs.

Scheme 1. Half-Reactions and the Overall Net Reaction in a Methanol Fuel Cell: (a) Protonic Half-Reactions in a Conventional Fuel Cell; (b) Reactions in an Alkaline Fuel Cell

(a)

Anode: $CH_3OH + H_2O \rightarrow CO_2 + 6\,e^- + 6\,H^+$

Cathode: $3/2\,O_2 + 6\,H^+ + 6\,e^- \rightarrow 3\,H_2O$

Net: $CH_3OH + 3/2\,O_2 \rightarrow CO_2 + 2\,H_2O$

(b)

Anode: $CH_3OH + 6\,OH^- \rightarrow CO_2 + 5\,H_2O + 6\,e^-$

Cathode: $3/2\,O_2 + 3\,H_2O + 6\,e^- \rightarrow 6\,OH^-$

Net: $CH_3OH + 3/2\,O_2 \rightarrow CO_2 + 2\,H_2O$

For example, poly(vinylidene fluoride) (PVDF) and poly(tetrafluoroethene-*co*-hexafluoropropylene) (FEP) have been grafted with 4-vinylbenzyl chloride, followed by modification of the benzyl chloride functionality with trimethylamine to give the trimethylbenzylammonium salt, which was then tested as an AAEM.[18] While the FEP-based AAEM gave conductivities of ca. 0.02 S/cm at ambient temperature and an atmospheric relative humidity of 100%, the PVDF-based AAEM degraded on subsequent amination and hydroxide ion exchange.

An important feature of AAEMs is that their conductivities are directly proportional to the ionophore densities. Commonly studied ionophores tethered to AAEM backbones are quaternary ammonium salts. However, these salts experience relatively intense cation−anion interactions, which further impede hydroxide ion mobility. Here we report the synthesis and characterization of a potentially improved AAEM that incorporates novel types of phosphonium cations as depicted in Scheme 2b,c. These ionophores have a reduced charge density due to their resonance structures that distribute the positive charge (Scheme 3) and thus diminish ionic interaction, which should facilitate hydroxide ion mobility.

These phosphonium side groups have been attached to Nafion (Scheme 2a), a tetrafluoroethylene copolymer bearing sulfonic

* Corresponding author. E-mail: srohr@iastate.edu.

10.1021/ma802613k CCC: $40.75
Published on Web 02/17/2009

Scheme 2. (a) Representation of the Average Chemical Structure of Nafion and Nafion-F; (b) Representation of Nafion Polymer Segments Attached to Proazaphosphatranium Functional Groups A^+; (c) Representation of the Same Nafion Polymer Segments Bonded to Phosphatranium Functional Groups B^+

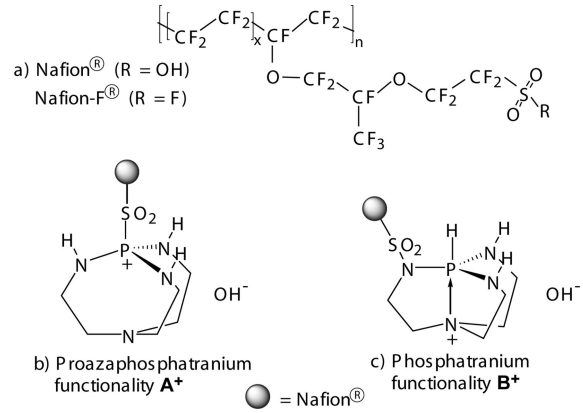

Scheme 3. Resonance Structures for a Proazaphosphatranium Cation

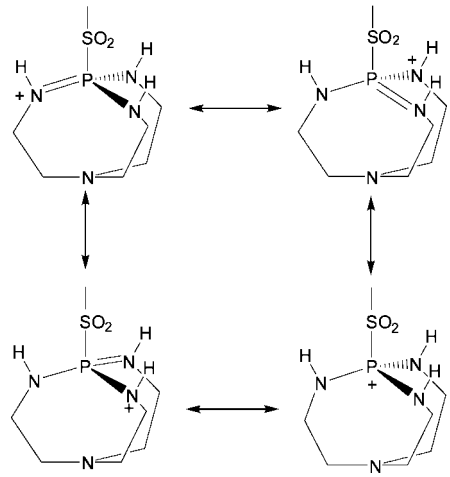

Scheme 4. Synthesis of Naf-Phan-X and Naf-Phan-OH

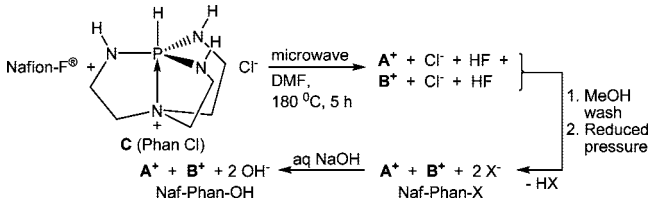

acid ($-SO_2OH$) functional groups which is extensively used as a PEM in fuel cells. Being perfluorinated and semicrystalline, Nafion (a proton cation conductor commercially derived via base hydrolysis of Nafion-F) and its precursor, Nafion-F (which contains $-SO_2F$ functionalities), possess good thermal and mechanical stability, which are particular advantages of Nafion compared with many other potential PEM materials. Nafion is stable up to 300 °C.[19] Its excellent conductivity stems from its combination of a hydrophobic polymer backbone and hydrophilic functional groups which self-organize to form water channels of ~2.5 nm diameter through which small ions can be easily transported.[20]

The synthesis steps for our material are summarized in Scheme 4, wherein Phan denotes the incorporation into the Nafion (Naf) polymer of the two structurally different types of phosphorus cations [i.e., proazaphosphatranium (A^+ in Scheme 2) and phosphatranium (B^+ in Scheme 2)] and "X" designates the anions Cl^- or F^-. Solid state nuclear magnetic resonance (NMR) is a promising tool for assessing the relative levels of A^+, B^+, or other functionalities incorporated and for detailing their chemical structure, since the material is rich in NMR-active spin-$^1/_2$ isotopes, namely ^1H, ^{13}C, ^{31}P, ^{19}F, and ^{15}N. The characteristic chemical shifts of the ^{31}P, ^1H, ^{13}C, and ^{15}N in Naf-Phan-X were detected in quantitative direct polarization (DP) experiments (for ^{31}P and ^{19}F) and in cross-polarization (CP) experiments (for ^{31}P, ^{13}C, and ^{15}N). The potential bonding of the three latter isotopes to hydrogen was determined by recoupling the dipolar interaction with ^1H. The correlations between phosphorus or carbon and their nearest protons were determined by 2D $^1H-^{31}P$ and $^1H-^{13}C$ heteronuclear correlation (HetCor) NMR. The bonding between Nafion and proazaphosphatranium/phosphatranium moieties was elucidated using $^{31}P\{^{19}F\}$ rotational-echo double resonance (REDOR).[25] ^{13}C spectra were edited with CH and CH_2 selection sequences[33,34] to identify such segments unambiguously.

Experimental Section

Samples. Nafion-F membrane (6 cm × 6 cm), with a 0.9 mmol/g loading of SO_2F functionality and a thickness of 25 μm (a product of Du Pont supplied by Ion Power Inc.), was charged to a microwave vial. To this was added excess phosphatranium chloride (Phan-Cl in Scheme 4; 500 mg, 2.3 mmol) prepared according to a literature method[21] and dry dimethylformamide (ca. 8 mL) such that the membrane was completely immersed in the solution. The mixture was microwaved at 180 °C for 5 h using a 300 W CEM Discover apparatus, and then the membrane was washed with copious amounts of methanol to remove any unreacted phosphatranium salt, HX, and solvent. For solid state NMR characterization, the Naf-Phan-X membrane was dried at room temperature under reduced pressure. For electrical measurements (to be reported in due course) the Naf-Phan-X membrane was soaked in aqueous NaOH to exchange the halide ions for hydroxide, giving Naf-Phan-OH in Scheme 4. The change in counterion is unlikely to result in significant structural changes of the polymer or side groups.

NMR Parameters. All NMR experiments were performed on a Bruker DSX-400 spectrometer at a resonance frequency of 400 MHz for ^1H, 100 MHz for ^{13}C, 162 MHz for ^{31}P, 376 MHz for ^{19}F, and 40.5 MHz for ^{15}N, using double-resonance or triple-resonance magic-angle spinning (MAS) probes. ^{13}C experiments were performed in 7 mm rotors at 6.5 kHz with 90° pulse lengths of 4 μs and 3 s recycle delays; ^{31}P experiments in 4 mm rotors at 7 kHz with 90° pulse lengths of 4 μs and either 2 s recycle delay for cross-polarization or 100 s for direct polarization; and ^{19}F experiments in 2.5 mm rotors at 30 kHz, which reduces ^{19}F dipolar couplings enough to resolve various side-group and backbone signals in Nafion, with 90° pulse lengths of 1.85 μs and 3 s recycle delays. ^{15}N experiments were performed in 7 mm rotors at 5 kHz with 90° pulse lengths of 9.2 μs and 2.5 s recycle delays; the number of scans was 6144 for phosphatranium chloride and 28 672 for Naf-Phan-X. Two-pulse phase modulation (TPPM) was used for $^1H-^{13}C$, $^1H-^{31}P$, or $^1H-^{15}N$ heteronuclear dipolar decoupling. ^{31}P and ^{15}N chemical shifts were indirectly referenced to H_3PO_4 and liquid NH_3, respectively, using hydroxyapatite (^{31}P chemical shift at +3 ppm) and *N*-acetylvaline (^{15}N chemical shift at +122 ppm). All experiments were carried out at ambient temperature.

$^1H-^{31}P$ and $^1H-^{13}C$ HetCor. Two-dimensional (2D) $^1H-^{31}P$ and $^1H-^{13}C$ heteronuclear correlation (HetCor) NMR experiments[22,23] were performed at spinning frequencies of 7 and 6.5 kHz, respectively. Frequency-switched Lee−Goldburg[24] homonuclear decoupling was applied during the evolution period t_1. Lee−Goldburg cross-polarization was used to suppress $^1H-^1H$ spin diffusion during polarization transfer and to show mostly one- and two-bond $^1H-^{13}C$ connectivities. For $^1H-^{31}P$ HetCor, the cross-polarization time was 0.7 ms, the number of scans was 128, and the number of t_1 increments was 100. For $^1H-^{13}C$ HetCor, the cross-polarization

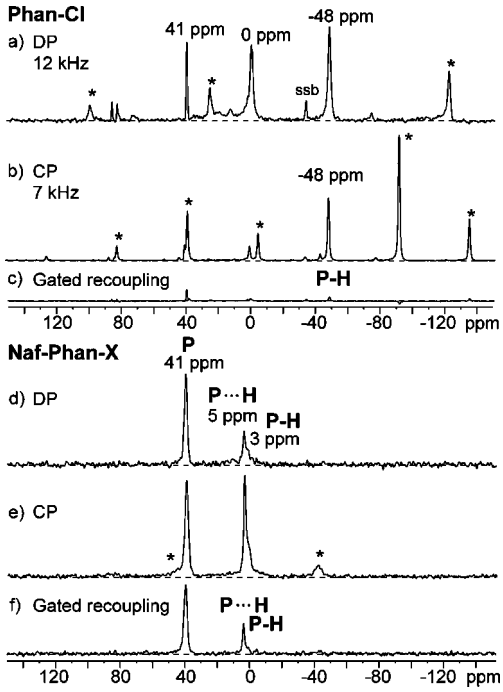

Figure 1. ^{31}P spectra of phosphatranium chloride (Phan-Cl, a−c) and Naf-Phan-X membrane (d−f). For Phan-Cl, (a) direct polarization (DP) at $\nu_r = 12$ kHz with a recycle delay of 100 s and (b) ^{1}H−^{31}P cross-polarization (CP) at $\nu_r = 7$ kHz with a recycle delay of 100 s show the centerband of the main ^{31}P signal with an isotropic chemical shift of −48 ppm; its spinning sidebands are labeled with asterisks. A sideband of the +41 ppm peak is labeled "ssb". (c) CP spectrum after gated recoupling for one rotation period, which confirms that the peak at −48 ppm is the signal of a protonated phosphorus. For the Naf-Phan-X membrane, the DP spectrum (d) at $\nu_r = 12$ kHz with a recycle delay of 100 s shows two resolved ^{31}P peaks (at 41 and ∼5 ppm) with an area ratio of 2:1. (e) CP spectrum at $\nu_r = 7$ kHz. Sidebands of the shoulder at 3 ppm are labeled by asterisks. (f) CP spectrum after gated recoupling for one rotation period.

time was 0.2 ms, the number of scans was 128, and the number of t_1 increments was 72.

$^{31}P\{^{19}F\}$ REDOR. $^{31}P\{^{19}F\}$ REDOR experiments[25] were performed in 2.5 mm rotors at a spinning frequency of 30 kHz, which avoids excessive dephasing losses and allows semiquantitative ^{31}P{^{19}F} distance measurements. The dephasing of ^{31}P magnetization in the field of the ^{19}F spins was observed. ^{19}F composite $90°x-180°y-90°x$ pulses of 7.6 μs duration were applied with pulse centers spaced by $t_r/2$ during a period of Nt_r in order to recouple the dipolar interaction between ^{31}P and ^{19}F. EXORCYCLE was used for the single 180° pulse on the ^{31}P channel.[26] The recoupling ^{19}F pulses were turned off to obtain the reference signal S_0.

Results and Discussion

^{31}P NMR: Chemical Bonding of Phosphorus. The ^{31}P MAS NMR spectra (Figure 1a,b) of phosphatranium chloride (Phan-Cl) show a dominant centerband at an isotropic chemical shift of −48 ppm with spinning sidebands (labeled with asterisks) spaced by the spinning frequency ω_r. The signal was quickly dephased by the H−P dipolar coupling during gated recoupling (see Figure 1c), as expected for a P−H group ("protonated phosphorus"). The ^{31}P chemical shift is close to the value of −43 ppm for the phosphatranium ion in solution as reported in the literature.[27] Peaks at 0 and +41 ppm must be assigned to impurities or more likely degradation products due to decomposition of Phan-Cl in the presence of water; these peaks do not appear in solution spectra of fresh Phan-Cl in organic solvents.[27] In the spectra of the product Naf-Phan-X (Figure 1d,e), two major peaks at +41 and ∼+5 ppm are observed,

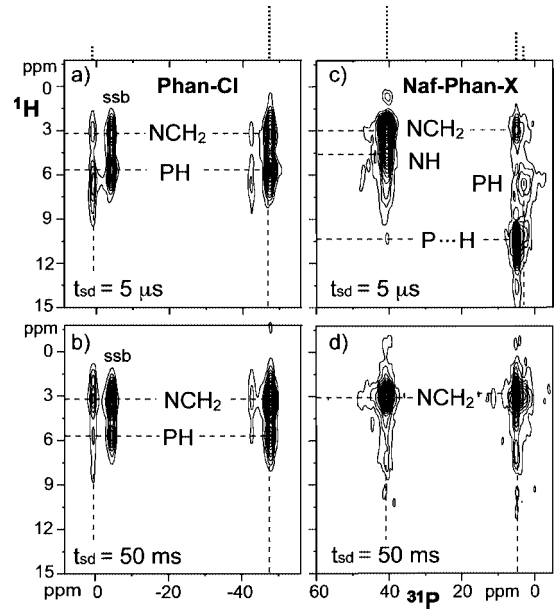

Figure 2. ^{1}H−^{31}P HetCor spectra of (a, b) phosphatranium chloride (Phan-Cl) and (c, d) Naf-Phan-X with a CP time of 0.7 ms and at $\nu_r =$ 7 kHz for mixing times of 5 μs and 50 ms. For Phan-Cl, the HetCor spectra show the centerband at −48 ppm in the ^{31}P dimension, a spinning sideband ("ssb") near −5 ppm, and an impurity peak at +1 ppm. The centerband positions are indicated by dashed lines at the top of the figure.

with an area ratio of 2:1 in the quantitative DP spectrum. The peak at 41 ppm is associated with a non-protonated phosphorus as indicated by slow CP and slow dephasing by gated recoupling (see Figure 1f). The peak near 5 ppm consists of two components (which are confirmed by ^{1}H−^{13}C correlation below): (i) a broader band centered at 3 ppm, with significant spinning sidebands, and fast H−P dephasing indicative of P bonded to H, and (ii) the peak at 5 ppm, which shows slower H−P dephasing that may suggest a phosphorus close to a proton but with a smaller H−P dipolar coupling due to a larger internuclear distance or motional averaging. The peak at 41 ppm is assigned to Naf-Phan-X of functionality $\mathbf{A}^+$. This assignment is proven below using ^{1}H−^{31}P HetCor spectra and further supported by chemical shift analysis. The peaks at ∼5 ppm can be tentatively assigned to the $\mathbf{B}^+$ functionality; the ∼3 ppm variation in chemical shifts might be due to different hydrogen bonding. According to the peak areas in the quantitative ^{31}P NMR spectrum, the Naf-Phan-X functionality $\mathbf{A}^+$ accounts for 67% of the total phosphorus content in our sample.

In order to identify ^{1}H near phosphorus, two-dimensional ^{1}H−^{31}P HetCor experiments (Figure 2) were performed with mixing times of 0.05 ms (nearest ^{1}H) and 50 ms (^{1}H within ∼3 nm). For phosphatranium chloride, the proton bonded to the phosphorus resonates at 5.6 ppm,[28] which is shown by the stronger cross-peak to the ^{31}P at −48 ppm and its spinning sideband in the spectrum of Figure 2a. In the spectrum after 50 ms of spin diffusion (Figure 2b), the cross-peaks for longer distance ^{1}H−^{31}P correlation, i.e., between phosphorus and protons in NH and NCH$_2$ groups (^{1}H chemical shift at ∼3 ppm), surpass those for the direct P−H bonding, due to their larger number. The ^{1}H band of protons in P−NH groups, whose chemical shift varies between ∼4 and 5.1 ppm in the literature,[27,28] is not clearly recognizable in the 2D HetCor spectra. For Naf-Phan-X, the phosphorus at 41 ppm correlates only to the NH and NCH$_2$ protons. The phosphorus at 5 ppm seems to be close to a proton at ∼10 ppm (Figure 2c), which might suggest a strongly H-bonded proton (P−H...X where X = O or N). This could occur in structure $\mathbf{B}^+$, wherein the presence of

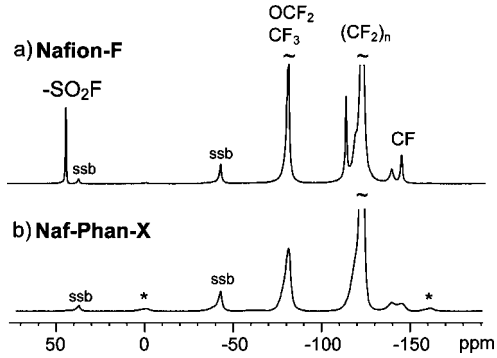

Figure 3. ^{19}F NMR spectra of (a) Nafion-F and (b) Naf-Phan-X by direct polarization at $\nu_r = 30$ kHz. The peak of the ^{19}F directly bonded to sulfur at +46.5 ppm in Nafion-F has disappeared in the Naf-Phan-X sample. In addition, the ^{19}F peaks of the Naf-Phan-X sample are broader than those of Nafion-F, which indicates reduced mobility. Spinning sidebands of the $(CF_2)_n$ peak are labeled "ssb" and those of the main side group signal by asterisks.

a five-membered −N−S−O−H−P− ring is conceivable. Further, a distinct set of cross-peaks is seen at +3 ppm in the ^{31}P dimension and ∼6 ppm in ^{1}H, assigned to P−H groups, confirming the presence of two components resonating near 5 ppm in the ^{31}P spectrum of Naf-Phan-X. It is interesting to note that an impurity with quite similar ^{31}P and ^{1}H chemical shifts is visible in the spectrum of Phan-Cl (see Figure 2a).

^{19}F and ^{31}P{^{19}F} REDOR NMR: Changes in the Nafion Side Chain. The ^{31}P NMR results have proven the change in phosphorus bonding from protonated to non-protonated for the primary product $\mathbf{A}^+$ in the Naf-Phan-X sample. ^{19}F NMR spectra (Figure 3) show that the fluorine in SO_2F groups in the precursor Nafion-F, which originally resonated at +46.5 ppm, have totally disappeared in the ^{19}F spectrum for Naf-Phan-X membrane. This confirms that Nafion side chains have reacted by losing a fluorine atom. In addition, the ^{19}F spectral lines have become broader, which indicates reduced mobility of the perfluoropolymer matrix,[29] likely due to attached large molecules.

^{31}P{^{19}F} REDOR experiments (Figure 4) were performed to confirm the bonding between the perfluoropolymer matrix and the proazaphosphatranium cations by estimating the distance between phosphorus and fluorine. Parts a and b of Figure 4 show ^{31}P{^{19}F} REDOR reference (S_0) and dephased (S) spectra, respectively, for Naf-Phan-X at $Nt_r = 1$ ms. The ^{31}P peak at 41 ppm, tentatively assigned to $\mathbf{A}^+$ functionality from ^{1}H−^{31}P spectra, was dephased to 50%, while the peak at 5 ppm (possibly associated with $\mathbf{B}^+$ from ^{1}H−^{31}P spectra) showed no significant dephasing. The REDOR experiment was also run at $Nt_r = 2$ ms, where the peak at 41 ppm had dephased to about 17% (circles in Figure 4c). The dephasing rate was compared to that of fluoroapatite, a crystalline mineral solid with a F−P distance of ∼0.36 nm[30] (triangles in Figure 4c). The dephasing of the phosphorus peak in Naf-Phan-X of functionality $\mathbf{A}^+$ is faster than for the phosphorus in fluoroapatite. This suggests an F−P distance comparable to ∼0.4 nm, which corresponds approximately to a three-bond fluorine−phosphorus distance. This is confirmed by REDOR simulations (see dashed lines in Figure 4c) of one ^{31}P spin coupled to many ^{19}F spins on a cubic lattice of 0.28 nm spacing (45 ^{19}F/nm^3), analogous to simulations described previously.[31,32] A time scaling factor of 0.73 was used, as determined from the fluoroapatite dephasing and consistent with the finite-pulse length effects (only 54% of a rotation period are without pulses). Adequate fits of the dephasing in Naf-Phan were obtained for a closest ^{31}P−^{19}F distance of 0.4 ± 0.1 nm. Thus, the 41 ppm feature is again consistent with the $\mathbf{A}^+$ functionality, while the 5 ppm feature matches the larger P−F distance of the $\mathbf{B}^+$ functionality.

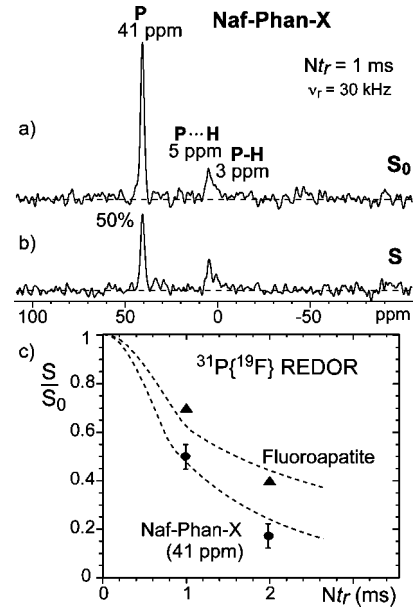

Figure 4. ^{31}P{^{19}F} REDOR spectra of Naf-Phan-X at $Nt_r = 1$ ms with recycle delay of 30 and 256 scans. (a) Reference spectrum (S_0) and (b) spectrum after recoupling (S) which shows dephasing for ^{31}P peak at 41 ppm of 50% but little, if any, dephasing for the peak at 5 ppm. (c) REDOR S/S_0 curve of Naf-Phan-X (circles) with comparison to fluoroapatite (triangles), which has an F−P distance of ∼0.36 nm. Dashed lines are simulation curves, with a closest ^{31}P−^{19}F distance of 0.4 nm for Naf-Phan-X (for further details see text).

^{1}H−^{13}C NMR: Structure of the Proazaphosphatranium Cation. To ensure that the primary structure of the phosphatranium chloride has not been altered during the synthesis of the Naf-Phan-X membrane, a set of one-dimensional NMR spectra with spectral editing[33,34] was recorded (Figure 5). For phosphatranium chloride, the ^{13}C spectra clearly show two NCH_2 signals, at 34 and 51 ppm. This assignment is confirmed by spectral editing that selects signals of CH_2 groups (see Figure 5c). The ^{13}C chemical shifts are in good agreement with literature values (see below). However, for Naf-Phan-X, four ^{13}C peaks were observed. In addition to signals at 54 and 46 ppm, assigned to NCH_2 groups of the proazaphosphatranium cations bonded to Nafion, additional bands are seen at 159 ppm, from a protonated carbonyl group (aldehyde, HC═O), and at 37 ppm, from a methyl group which persists in the spectrum after gated decoupling due to motional averaging of C−H coupling by fast uniaxial rotation. The carbonyl and methyl groups are most likely from dimethylformamide (DMF), the swelling agent used, which may be trapped in the membrane. The structure and solution state ^{13}C chemical shifts of DMF are shown in Figure 5. As expected, in the ^{1}H−^{13}C HetCor spectra (Figure 6) the carbonyl carbon correlates to a proton at ∼8 ppm, and all other carbons correlate to NCH_n protons at ∼3 ppm. Interestingly, one methyl group of DMF, which resonates at 31.3 ppm, is not observed in the ^{13}C spectra of Naf-Phan-X. The second correlation of the 159 ppm ^{13}C resonance to a ^{1}H at 3 ppm is consistent with a more distant coupling to NCH_n protons, as confirmed by its relative prominence with a longer delay for spin diffusion (see Figure 6b).

^{15}N NMR. The ^{15}N NMR spectrum of phosphatranium chloride obtained by cross-polarization from ^{1}H (Figure 7) shows a peak at 50 ppm (referenced to liquid NH_3) from protonated nitrogen and a peak at 37 ppm from non-protonated (tertiary) nitrogen, so assigned due to signal persistence in the CP/gated experiment (see Figure 7b). A small signal is also observed at 23 ppm, but due to limited sensitivity it is uncertain whether

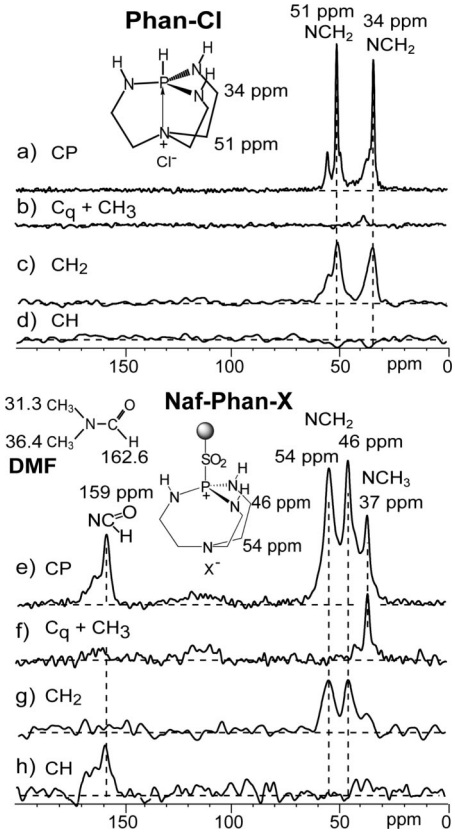

Figure 5. ^{13}C spectra of phosphatranium chloride (Phan-Cl, a−d) and Naf-Phan-X membrane (e−h). (a, e) CP and (b, f) CP/gated decoupling experiments, run at $\nu = 6.5$ kHz. (c, g) CH_2 and (d, h) CH selection experiments at $\nu_r = 5.787$ kHz. For phosphatranium chloride, two peaks of CH_2 bonded to nitrogen are seen at 34 and 51 ppm. For Naf-Phan-X, the two CH_2 peaks shift to 46 and 54 ppm, respectively. In addition, a protonated carbonyl group and a nitrogen-bonded methyl group are present in a ~1:1 ratio. These are most likely from the swelling agent *N,N*-dimethylformamide (DMF) trapped in the membrane. The structure of DMF is shown, with solution state ^{13}C chemical shifts indicated.

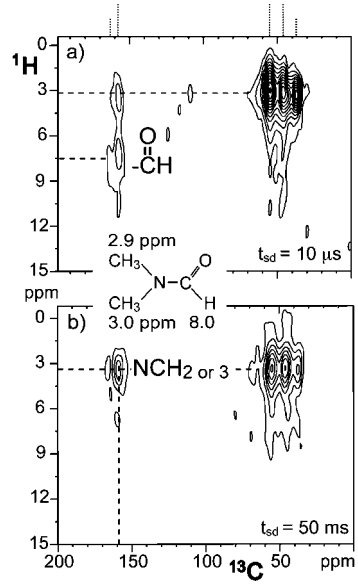

Figure 6. $^{1}H-^{13}C$ HetCor spectra of Naf-Phan-X with spin-diffusion times of (a) 10 μs and (b) 50 ms at $\nu_r = 6.5$ kHz. ^{13}C signal positions are indicated by dashed lines at the top of the figure. Solution state ^{1}H NMR chemical shifts for DMF are shown with the structure.

this is protonated or not. The relative peak areas are 1.6:1:0.5, which does not match the expected 3:1 ratio. However, it should

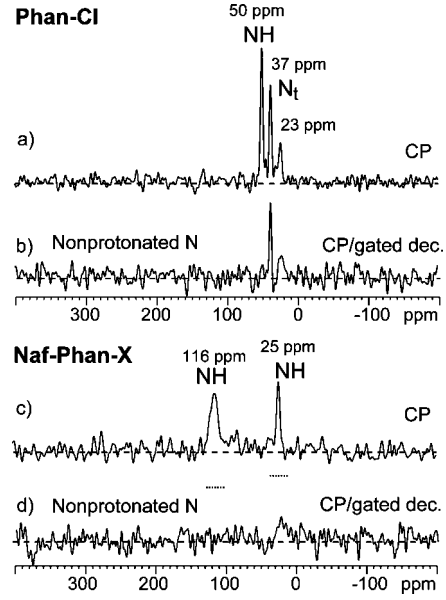

Figure 7. ^{15}N spectra of phosphatranium chloride (a, b) and Naf-Phan-X (c, d) obtained after CP and CP with recoupled gated decoupling, respectively; $\nu_r = 5$ kHz. Dashed horizontal lines in (d) mark the intensity expected if the N observed in (c) was not protonated.

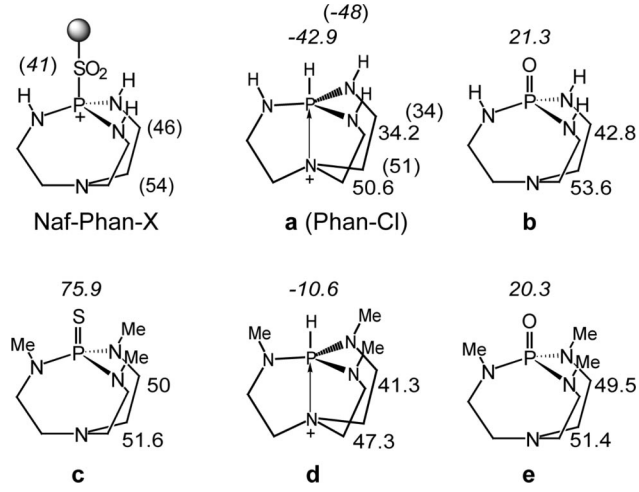

Figure 8. Chemical shifts of structures similar to phosphatranium chloride from ref 27. ^{31}P chemical shifts are in italics, while ^{13}C chemical shifts are in regular font. The results from our experiments are given in parentheses.

be noted that a significant level of degradation products are detected in the ^{31}P spectrum of this sample (see Figure 1a), and similar degradation might account for the 23 ppm ^{15}N resonance. The signal of the protonated nitrogen has been shifted to 25 ppm in the spectrum for Naf-Phan-X (Figure 7c). No peak of non-protonated nitrogen is seen, which may be due to low cross-polarization efficiency of this tetracoordinated nitrogen strongly diluted in the polymer matrix; the cross-polarization condition may have shifted due to power absorption by the slightly conductive sample. The ^{15}N peak at 116 ppm can be assigned to an amide (N−C═O) structure; it may come from DMF, but the nitrogen appears to be protonated (HN−C═O).

Analysis of Chemical Shifts. In Figure 8, literature chemical shift values[27] of ^{31}P (in italics) and ^{13}C (in regular font) are listed for phosphatranium chloride and its derivatives. For phosphatranium chloride, the literature values agree well with the results from our experiments (given in parentheses). Though none of the derivatives have the same structure as Naf-Phan-X, we can analyze them to obtain insights into chemical shift trends.

For example, substituting the proton on phosphorus by a sulfur (from structure **d** to **c**) changes the ^{31}P chemical shift by +87 ppm, which is similar to the change by +89 ppm from phosphatranium chloride to the chemical shift assigned to the proazaphosphatranium functionality $\mathbf{A}^+$ in Naf-Phan-X. In addition, the similar ^{13}C chemical shifts for structures **b**, **c**, **e** and Naf-Phan-X may indicate elongation of the cagelike molecular structure of the proazaphosphatranium functionality $\mathbf{A}^+$ in Nafion-Phan-X. Such elongation is relative to structures **a** (Phan-X) and **d** of Figure 8, with their shorter P−N distances due to transannular donation of a nitrogen lone pair to phosphorus. This bonding yields correspondingly unique ^{13}C shifts and a P−N distance of ∼0.2 nm, in contrast to ∼0.3 nm for structures **b**, **c**, and **e**,[35] whose ^{13}C shifts are more akin to the Naf-Phan-X system.

Structural Implications. The new AAEM possesses several interesting features which we now discuss. Resonance structures of proazaphosphatranium cations of type $\mathbf{A}^+$ in Scheme 2b can distribute the positive charge in the P−N bonds surrounding the phosphorus (Scheme 3). Such resonance structures minimize Coulombic attractions between the cations and anions and hence can improve the mobility of the anion. It is interesting that analogous cations representative of $\mathbf{A}^+$ and $\mathbf{B}^+$ (i.e., $[-CS(O)_2P(N-)_3]^+$ and $[-CS(O)_2N(C)P(N-)_2]^+$, respectively) are, to our knowledge, completely unprecedented in the literature. The robust mechanical, oxidative, hydrolytic, and thermal stability of the Nafion framework, the diffuse distribution of positive charge, and hydrolytic stability of 4-coordinate proazaphosphatranium and 5-coordinate phosphatranium cations are combined in the novel "hybrid" AAEM depicted in Scheme 2. Thus, we have in a formal sense transformed Nafion from a PEM material into a halogenide- and a hydroxide-containing AAEM. We accomplished this "ion polarity inversion" of Nafion by a simple experimental procedure using commercially available Nafion-F as shown in Scheme 4. The Naf-Phan-OH film may be an excellent candidate in AFC fuel cell applications according to preliminary studies, showing that it retains good conductivity under strongly basic conditions as well as at elevated temperatures.

Conclusions

A Nafion−proazaphosphatranium/phosphatranium composite cationic film, a potential anion exchange membrane for direct methanol-based fuel cells, was successfully synthesized via a microwave process from Nafion-F and phosphatranium chloride. Most of the latter was converted to proazaphosphatranium cations attached to the Nafion via a PS bond (structure $\mathbf{A}^+$), as shown by $^{31}P\{^1H\}$, ^{19}F, and $^{31}P\{^{19}F\}$ REDOR NMR. These ionophores have a reduced charge density due to resonance structures that distribute positive charge to diminish ionic interaction, which should facilitate hydroxide ion mobility. Electrical measurements to complement the present structural study and further test these hypotheses are underway. The 4-coordinate stereochemistry of phosphorus in the novel proazaphosphatranium cation was substantiated by ^{13}C and ^{15}N NMR. About one-third of the phosphatranium ions are converted into two other structures, with S not bonded to P but most likely to N as in structure $\mathbf{B}^+$. In addition, moieties derived from the solvent DMF were found in the final product. Efforts to inhibit formation of these impurities are underway.

Acknowledgment. Work by X.K. and K.S.-R. at the Ames Laboratory was supported by the Department of Energy Basic Energy Sciences under Contract DE-AC02-07CH11358. Work by K.W. and J.G.V. was supported by the Department of Defense AFRL under Contract FA8650-05-C-2541.

References and Notes

(1) Chu, D.; Jiang, R. *Solid State Ionics* **2002**, *148*, 591.
(2) Dyer, C. K. *J. Power Sources* **2002**, *106*, 31.
(3) Chang, H.; Kim, J. R.; Cho, J. H.; Kim, H. K.; Choi, K. H. *Solid State Ionics* **2002**, *148*, 601.
(4) Meyers, J. P.; Maynard, H. L. *J. Power Sources* **2002**, *109*, 76.
(5) Eye for Fuel Cells Conference on Fuel Cells for Portable Applications, Hilton Back Bay, Boston, MA, Sept 5−6, **2002**.
(6) Ren, X.; Zelenay, P.; Thomas, S.; Davey, J.; Gottesfeld, S. *J. Power Sources* **2000**, *86*, 111.
(7) Raadschelders, J. W.; Jansen, J. *J. Power Sources* **2001**, *96*, 160.
(8) Varcoe, J. R.; Slade, R. C. T. *Fuel Cells* **2005**, *5*, 187.
(9) Lamy, C.; Belgsir, E. M.; Leger, J.-M. *J. Appl. Electrochem.* **2001**, *31*, 799.
(10) Tripkovic, A. V.; Popovic, K. D.; Grgur, B. N.; Blizanac, B.; Ross, P. N.; Markovic, N. M. *Electrochim. Acta* **2002**, *47*, 3707.
(11) Yu, E. H.; Scott, K.; Reeve, R. W. *J. Electroanal. Chem.* **2003**, *547*, 17.
(12) Gamburzev, S.; Petrov, K.; Appleby, C. L. *J. Appl. Electrochem.* **2002**, *32*, 805.
(13) Wagner, N.; Schulze, M.; Gulzow, E. *J. Power Sources* **2004**, *127*, 264.
(14) Schulze, M.; Gulzow, E. *J. Power Sources* **2004**, *127*, 252.
(15) McLean, G. F.; Niet, T.; Prince-Richard, S.; Djilali, N. *Int. J. Hydrogen Energy* **2002**, *27*, 507.
(16) Schulze, M.; Gulzow, E. *J. Power Sources* **2004**, *127*, 243.
(17) Cifrain, M.; Kordesch, K. V. *J. Power Sources* **2004**, *127*, 234.
(18) Danks, T. N.; Slade, R. C. T.; Varcoe, J. R. *J. Mater. Chem.* **2002**, *12*, 3371.
(19) Sun, L.; Thrasher, J. S. *Polym. Degrad. Stab.* **2005**, *89*, 43.
(20) Schmidt-Rohr, K.; Chen, Q. *Nat. Mater.* **2008**, *7*, 75.
(21) Laramay, M. A. H.; Verkade, J. G. *Z. Anorg. Allg. Chem.* **1991**, *605*, 163–174.
(22) Bielecki, A.; Burum, D. P.; Rice, D. M.; Karasz, F. E. *Macromolecules* **1991**, *24*, 4820.
(23) Clauss, J.; Schmidt-Rohr, K.; Spiess, H. W. *Acta Polym.* **1993**, *44*, 1.
(24) Bielecki, A.; Kolbert, A. C.; de Groot, H. J. M.; Griffin, R. G.; Levitt, M. H. *Adv. Magn. Reson.* **1990**, *14*, 111.
(25) Gullion, T.; Schaefer, J. *J. Magn. Reson.* **1989**, *81*, 196.
(26) Sinha, N.; Schmidt-Rohr, K.; Hong, M. *J. Magn. Reson.* **2004**, *168*, 358.
(27) Galasso, V. *J. Phys. Chem. A* **2004**, *108*, 4497–4504.
(28) Reddy, C. R. V.; Verkade, J. G. *J. Org. Chem.* **2007**, *72*, 3093.
(29) Chen, Q.; Schmidt-Rohr, K. *Macromolecules* **2004**, *37*, 5995.
(30) Nikcevic, I.; Jokanovic, V.; Mitric, M.; Nedic, Z.; Makovec, D.; Uskokovic, D. *J. Solid State Chem.* **2004**, *177*, 2565.
(31) Rawal, A.; Wei, X.; Akinc, M.; Schmidt-Rohr, K. *Chem. Mater.* **2008**, *20*, 2583.
(32) Schmidt-Rohr, K.; Rawal, A.; Fang, X.-W. *J. Chem. Phys.* **2007**, *126*, 05401 (1−16).
(33) Schmidt-Rohr, K.; Mao, J.-D. *J. Am. Chem. Soc.* **2002**, *124*, 13938.
(34) Mao, J.-D.; Schmidt-Rohr, K. *J. Magn. Reson.* **2005**, *176*, 1.
(35) Verkade, J. G. New Aspects of Phosphorus Chemistry II. *Top. Curr. Chem.* **2002,** *233*, 1.

MA802613K